FIBER-OPTIC STRAIN GAUGE CALIBRATION AND DYNAMIC FLEXIBILITY TRANSFER FUNCTION IDENTIFICATION IN MAGNETIC BEARINGS

Zachary S. Zutavern, Dara W. Childs
Texas A&M University, Turbomachinery Laboratory
Department of Mechanical Engineering, MS 3123, College Station, TX 77843-3123
zsz@tamu.edu

ABSTRACT

Historical attempts to measure forces in magnetic bearings (MBs) have experienced limited success as a result of relatively high uncertainties. Recent advances in strain-gauge technology have provided a new method for measuring MB forces. Fiber-optic strain gauges (FOSGs) are roughly 100 times more sensitive than conventional strain gauges and are not affected by electro-magnetic interference. At the Texas A&M University (TAMU) Turbomachinery Laboratory, installing FOSGs in MBs has produced force measurements with low uncertainties. Dynamic flexibility transfer functions (DFTFs) exhibiting noticeable gyroscopic coupling have been identified and compared with finite element predictions. Comparison has verified the effectiveness of using MBs as calibrated exciters in rotordynamic testing. Many applications including opportunities for testing unexplained rotordynamic phenomena are now feasible.

INTRODUCTION

Research in rotordynamics, as in other fields, relies heavily on test measurements to characterize dynamic phenomena. Rotor and housing motions are measured with proximity probes, accelerometers, and occasionally velocimeters. These measurements can typically be determined accurately and with relative ease as compared with force measurements. Forces are typically measured with strain gauges and calibrated load cells, or they are calculated from inertial properties and accelerations. Clearly, it can be challenging to determine the force directly applied to a spinning rotor.

MBs have been recognized for years as having a great potential for force measurement. The non-contact bearing-rotor interface provides a method for applying forces directly to a rotating component. The applied force is a function of the air gap, the control current, and the magnetic properties of the materials. There have been attempts to determine the applied forces through modeling the magnetic force, measuring the magnetic flux, and by installing load cells within the bearings. However, the levels of uncertainty in such attempts have proved excessive.

Traxler and Schweitzer [1] mounted piezoelectric load cells between the interface of the magnetic bearing housings and the test platform to measure reaction forces. The force measurements were adjusted to compensate for bearing housing inertial forces to determine the force applied directly to the rotor. Lee, Ha, and Kim [2] used a similar approach to perform system identification. Both experienced large uncertainties associated with load cell flexibility and sensitivity.

Matros, Sobotzik, and Nordmann [3] used an empirical formula relating the bearing currents and the rotor position to the applied force. They also modeled hysteresis and saturation properties to improve results. A test rig was designed to identify the bending stiffness of a clamped beam. The stiffness measured by the MBs was 8% higher than the stiffness identified by a calibrated load cell. Fittro, Baun, Maslen, and Allaire [4] used an empirical formula to measure forces on a static test rig, varying eccentricity and force amplitude. They found that eccentricity changes contributed to most of the uncertainty in the results. The mean error distribution and standard deviation were 1% and 4% of the bearing load capacity respectively.

Gahler [5] used Hall sensors to measure the magnetic flux from the bearing poles. The rotor position and the magnetic flux were related to the force with an empirical formula. A correction algorithm was implemented to correct for eddy currents, hysteresis, and saturation. Dynamic forces were applied at

frequencies from 20 to 200 Hz with constant amplitude, and the force error was ±11% of load capacity. Dynamic forces were then applied at 120 Hz for various amplitudes, and the force error was reduced to ±2% of load capacity. Knopf and Nordmann [6] used flux measurements to identify dynamic properties of hydrodynamic bearings. Uncertainties were around 1% of load capacity for static measurements, but they deteriorated to 5% with increasing eccentricity and rotor speed.

Pottie [7] used several methods to determine forces of magnetic bearings. An empirical force model was used, and considerable time and effort were spent mapping the model coefficients. The Hall sensor approach was also attempted. Pottie also tried to measure forces by supporting the MB poles (not the bearing housings) with load cells. However load cells with sufficient sensitivity were relatively flexible and allowed the MB poles to move. Unfortunately, this introduced new vibration modes and resonances. Accelerometers were installed to compensate for the pole inertial forces. None of these attempts were able to significantly improve uncertainties over previous methods.

Recent efforts at the TAMU Turbomachinery Laboratory have focused on a new method of measuring forces in magnetic bearings. Strain sensors utilizing fiber-optic Fabry-Perot interferometery produce highly accurate measurements while remaining insusceptible to electromagnetic interference. By installing these highly sensitive strain gauges in magnetic bearings, accurate force measurements can be produced. Raymer and Childs [8] used FOSGs to measure dynamic forces applied by an external exciter. This method resulted in dramatic improvements in uncertainty, 1 lb (4 N) or .13% of the bearing load capacity.

Pavesi and Childs [9] attempted to use an empirical formula based on current and position to calibrate the FOSGs. The forces calculated from the formula were believed to be sufficiently accurate to calibrate at low frequencies. This method encountered difficulties associated with low force levels, and the resulting uncertainties were larger than those obtained by Raymer and Childs.

In the present work, a new calibration method has been developed and used to determine system properties. The new calibration method uses dynamic force calculations based on the mass properties of the rotor to calibrate the FOSGs. Using the calibrated FOSGs, DFTFs have been experimentally determined and compared with results from a finite element model. The details of the calibration and the DFTF identification comprise the remainder of this paper.

TEST RIG DESCRIPTION

The test rig consists of a rotor supported by radial magnetic bearings. The rotor is driven by an electric motor, and the system is equipped with pneumatic brakes. The FOSGs are installed in the non-drive end bearing. Data from the MB control system and the FOSG signal conditioning unit (SCU) are acquired using National Instruments (NI) hardware and Labview software. A detailed description of the test rig and data acquisition system follows.

Figure 1 displays a side view of the test rig. The magnetic bearings (1) have a load capacity of 800 lb (3560 N) and a span of 40 in. (1.02 m). They support a 60 in. (1.52 m) steel rotor (2) weighing 400 lb (1780 N). Disks (3) increase the polar inertia and, accordingly, the gyroscopic coupling. The laminate sleeves (4) mount to the rotor via a taper-induced interference fit. Auxiliary bearings (5) support the rotor

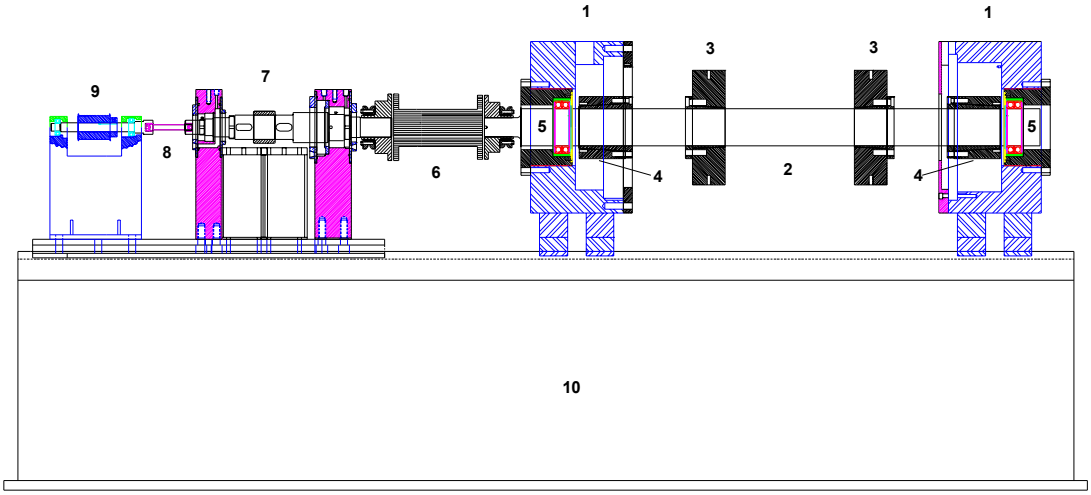

FIGURE 1: MB test rig at TAMU Turbomachinery Laboratory

when it is not levitated. The coupling (6) and the quill shaft (8) are both shielded for safety. The brakes (7) can be used to rapidly decelerate the rotor if the MB control system signals a fault. A pulley (9) and drive belt transmit power from the motor. The test stand (10) is constructed of .75 in. (19 mm) steel plates with a 3 in. (76 mm) thick steel top.

Four FOSGs are installed in the non-drive end MB. Each FOSG is bonded to the surface of one pole of each axis. The FOSGs are located near the tip of the pole as shown in Figure 2. Fiber-optic cables run from the FOSGs to the SCU. The SCU produces analog voltage outputs with voltage change proportional to changes in strain. For dynamic strains above 2 Hz, the FOSGs have a noise floor of less than .010 με.

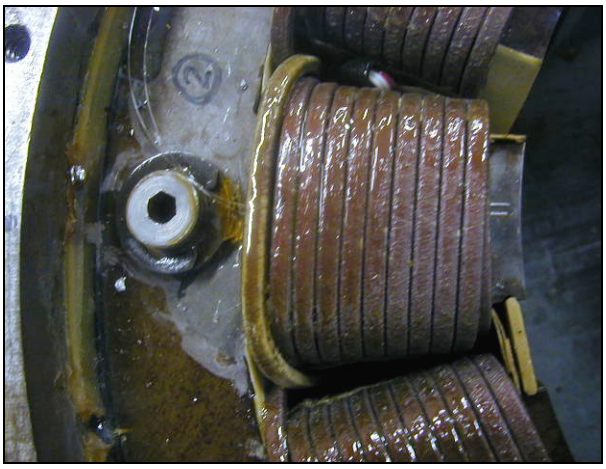

FIGURE 2: FOSG location

Analog outputs from the FOSG SCU and the measurement panel of the MB control system connect to an NI DAQ system. The system can simultaneously sample 16 analog inputs (16 bit) at 10 kHz and generate 4 analog output signals at 5 kHz. The DAQ hardware interfaces with a destop PC where Labview is used for waveform generation and signal analysis. The analog outputs are used to control the rotor target position to excite the rotor with the desired waveforms.

FOSG CALIBRATION

The calibration of the FOSGs has been accomplished in three ways. A low frequency external force, measured by a load cell, can be applied to the rotor. The FOSGs can then be calibrated with measurements from the load cell. The rotor can be excited at low frequencies, and the force calculated from an empirical formula can be used to calibrate the FOSGs. The rotor can also be excited at higher frequencies, and the rotor position measurements and mass properties can be used to calculated a force used in calibrating the FOSGs. The first method has proved successful but time consuming and impractical in field applications. The second method has not produced an accurate calibration because the low frequency requirement creates a poor force signal to noise ratio. The third method has been successfully implemented and will now be described more thoroughly.

The rotor is excited at both ends (in phase) horizontally and vertically, using single frequency excitations from 15 to 65 Hz in increments of 5 Hz. Rotor position measurements are obtained from the MB control system. Low frequency seismic accelerometers capable of detecting 1 μg at frequencies as low as .1 Hz are located on the bearing housings. The bearing housing accelerations are converted to position changes using the excitation frequency assuming sinusoidal motion. The bearing motion measurements are combined with the rotor position measurements to determine the rotor's absolute position. The absolute position measurements are analyzed by a finite element model to obtain calculated forces. The model is displayed in Figure 3. The calculated forces are correlated with the FOSG voltage response at the various calibration frequencies to obtain the FOSG calibration.

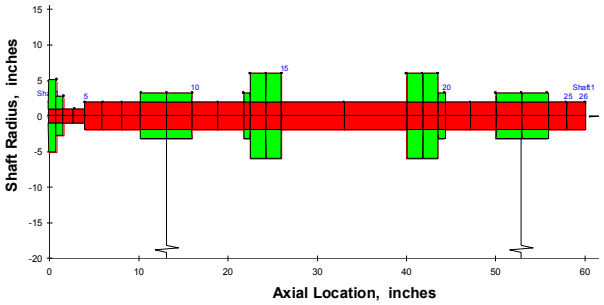

FIGURE 3: FE rotor model

In developing the calibration method, an unexpected effect was observed. As expected, the FOSG response exhibited an increase proportional to the square of the excitation frequency; however, the FOSG response also contained a frequency independent, position dependent strain (PDS). In fact, noticeable strain changes can be observed at frequencies low enough to neglect the inertial force of the rotor. The physical mechanism causing the strain change is not well understood. It likely results from changes in the magnetic field that occur for different radial rotor positions. The phase of the PDS is roughly 180° out of phase with the rotor position. The PDS amplitude is small relative to the strain at high calibration frequencies. The PDS is determined at low frequencies and subtracted from the FOSG response for the calibration. Figure 4 shows the PDS amplitude as a

function of position amplitude for two strain gauges S1 and S2. These results were obtained by exciting the rotor at the non-drive end bearing with a frequency of 3 Hz and amplitudes varying from 2 to 35 µm. The motion is perpendicular to the S1 axis and parallel to the S2 axis.

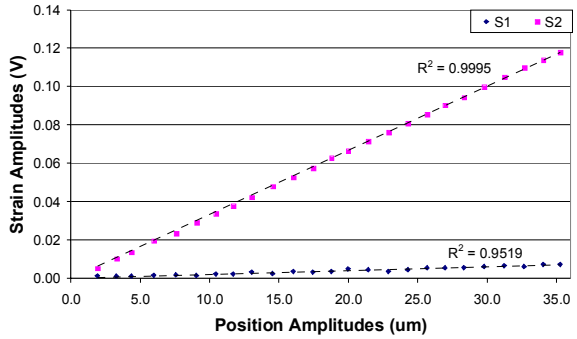

FIGURE 4: FOSG PDS

Another unexpected effect is calibration drift. If calibrations are repeated in close succession, the results demonstrate a high degree of repeatability. However, if several hours or days pass between the calibrations, an apparently random drift occurs. The drift that occurs over long periods of time is larger than the uncertainties exhibited during a given calibration. Consequently, calibration is preformed immediately before each test (testing is described in the following section). Typically, the calibration is repeated after the test for verification. Initially, temperature changes were blamed for the calibration drift. However, the dynamic nature of the calibration makes the calibration accuracy susceptible to FOSG sensitivity changes, but not to thermal related strain. The manufacturer of the FOSG reports only very slight sensitivity changes for a temperature change of 360° F (200° C). This property eliminates the effect of temperature on the FOSGs as a cause, because the temperatures for the test rig vary only slightly, from 75° to 90° F (24° to 32° C). Further efforts in isolating the cause of the calibration drift are warranted.

The uncertainty for a given calibration is 1 lb (4 N) or .13% of load capacity. The uncertainty for a given test is characterized by a comparison of calibrations taken before and after the test. For two calibrations taken 30 minutes apart (sufficient time for testing), the uncertainty is 2 lb (9 N) or .25% of load capacity. This uncertainty exhibits significant improvements over that of previous methods. However, by better understanding the PDS and the calibration drift, the uncertainty could likely be further reduced. These effects are of primary interest and are currently under investigation.

DFTF IDENTIFICATION

With a successful calibration prodecure, a variety of rotordynamic phenomena can be tested. Test programs can now utilize MBs as calibrated exciters and perform parameter identification of rotor properties or determine seal coefficients and even impeller coefficients. A less demanding rotordynamic test has been performed to validate the MB test methodology. By identifying DFTFs, results such as rotor-speed-dependent natural frequencies can be compared with predictions from the finite element model to validate the test method.

The DFTFs are determined from multiple tests using the FOSG force measurements and the MB control system position measurements. At each frequency, the flexibility matrix *G* is determined from a vertical and a horizontal excitation, as shown in Equation 1. The subscripts of the flexibility matrix elements indicate the force direction and the response direction respectively. Combining the flexibility matrices over the desired frequency range and repeating the tests at various rotor speeds produces the DFTFs.

$$\begin{bmatrix} G_{xx} & G_{yx} \\ G_{xy} & G_{yy} \end{bmatrix} = \begin{bmatrix} x_x & x_y \\ y_x & y_y \end{bmatrix} \begin{bmatrix} F_{xx} & F_{xy} \\ F_{yx} & F_{yy} \end{bmatrix}^{-1} \qquad (1)$$

The DFTFs are determined from 80 to 180 Hz. Frequency spacing is varied to emphasize results near the first bending mode of the rotor. The rotor is excited vertically and horizontally at the non-drive end bearing with shake amplitudes of 10 µm. DFTFs are computed for rotor speeds of 0 to 5000 rpm by 1000 rpm increments. Uncertainties are determined based on standard deviations of 10 repeated tests at 0 rpm.

Figures 5 and 6 display the amplitude and phase of the direct term G_{xx}. The other direct term G_{yy} exhibits similar characteristics. Figures 7 and 8 display the cross-coupled term G_{xy}. G_{yx} also exhibits similar characteristics. The uncertainties are displayed by the standard deviations plotted on the frequency axes.

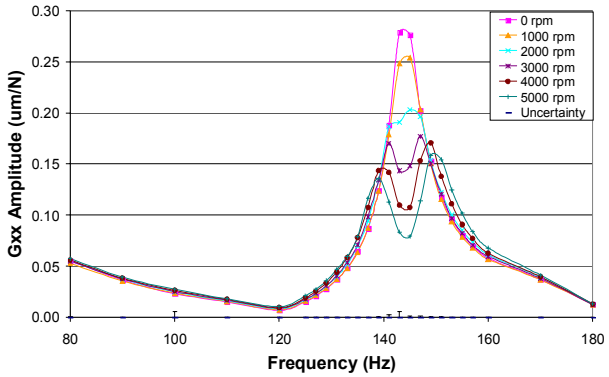

FIGURE 5: G_{xx} amplitude plot

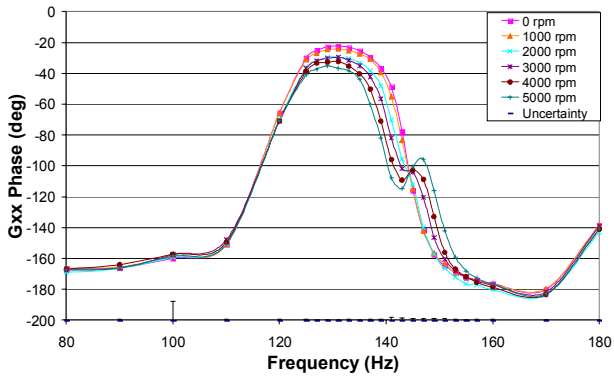

FIGURE 6: G_{xx} phase plot

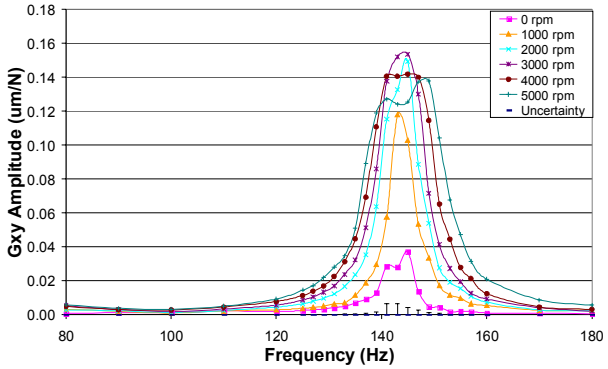

FIGURE 7: G_{xy} amplitude plot

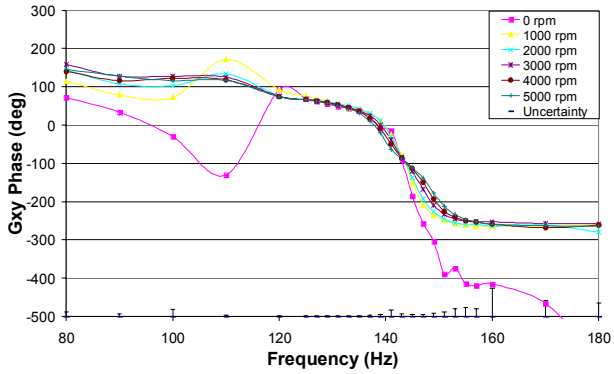

FIGURE 8: G_{xy} phase plot

CONCLUSIONS

The results contain peak responses corresponding to forward and backward natural frequencies. Response at the backward natural frequency appears because the exciting force is the vertical or horizontal sinusoid produced by the MBs. The results display significant cross-coupling with increasing rotor speed, most noticeably around the natural frequencies. The natural frequencies have separated by over 10 Hz at 5000 rpm. Figure 9 displays the damped natural frequency map from the finite element model. The predicted natural frequency separation at 5000 rpm is slightly more than 10 Hz. The finite element model predictions have a strong correlation with the results of DFTF tests.

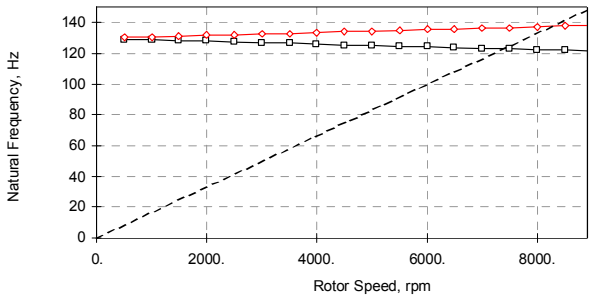

FIGURE 9: Damped natural frequency map

Uncertainties in the DFTFs tend to be lower where flexibility is low and higher where flexibility is high. This is because the excitation force levels are very low in regions of high flexibility. In general, the amplitude uncertainties are very good, and the DFTF curve uniformity reflects this. The phase uncertainty is somewhat more noticeable. The curves of the cross-coupled phases are not as smooth as might be expected based on the uncertainties. One possible cause of this could be the PDS correction. For low strain levels, phase error encountered during PDS subtraction would have a significant effect on the resulting corrected strain values. Consider two vectors of slightly different magnitude directed in roughly the same direction. Small uncertainties in the direction of either vector could have a noticeable effect on the direction of the difference between the vectors. The cross-coupled phases probably have larger uncertainties than detected by the standard deviation analysis. However, uncertainties given for the amplitudes of the direct and cross-coupled terms and for the phase of the direct term are indicative of the actual uncertainties. The results of the DFTF testing are encouraging and offer support for the application of FOSG force measurements in MBs to other areas of rotordynamics. These results demonstrate that FOSGs in MBs can accurately test rotodynamic properties of a system.

SUMMARY AND EXTENSIONS

Recent advances in strain gauge technology have provided an effective means of obtaining MB forces. After exploring several methods for calibrating the FOSGs, a calibration method has been developed that produces force measurements with uncertainties of .25% of the bearing load capacity. The calibrated FOSGs were successfully used to determine DFTFs. The experimental DFTFs exhibit a strong correlation

with results from the finite element model. This experiment has validated the potential use of MBs in rotordynamic testing.

Throughout calibration and testing, unexpected effects were encountered. The PDS has been addressed, and its effects have been reduced, but its cause has not been determined. Several possible causes have surfaced, but they have not yet been verified. The uncertainties in the FOSG calibration and the DFTF testing are acceptable for typical rotodynamic testing. However, considering the excellent repeatability of position measurements and the sensitivity of the FOSGs, the uncertainties can likely be further improved.

Other potential sources of uncertainty include the FOSGs and the condition of the MBs. The FOSGs have not been thoroughly tested by the manufacturer at the strain levels observed during testing and calibration. The bearing laminates exhibit signs of age such as delamination and slight corrosion. These factors may also have an impact on uncertainty. While further reduction of uncertainty is desirable, the present levels are acceptable for rotordynamic testing.

FOSG force measurements can now be applied in situations where the results and their physical causes are not well known or theoretically understood. MBs can be used as calibrated exciters to study new areas of rotordynamics. One such use is in determining impeller coefficients for compressors. MBs already installed in these compressors could be equipped with FOSGs, and the impeller forces could be measured. The potential applications of FOSGs in magnetic bearings are considerable, and the possibility for exploring new phenomena in rotordynamics is promising.

REFERENCES

[1] Traxler A., Schweitzer G., 1984, *Measurement of the Force Characteristics of a Contactless Electromagnetic Rotor Bearing*, Institute for Mechanics, ETH Zurich, Switzerland.

[2] Lee C., Ha Y., Kim C., 1994, "Identification of Active Magnetic Bearing System Using Magnetic Force Measurement," *The Fourth International Symposium on Magnetic Bearings*, Zurich, pp 305-309.

[3] Matros M., Sobotzik J., Nordmann R., 1998, "A New Model-Based Method for the Accurate Measurement of Magnetic Bearing Forces," microfiches, *Fourth International Symposium on Magnetic Suspension Technology*, Gifu City, Japan, pp 239-248.

[4] Fittro R., Baun D., Maslen E., Allaire P., 1997, "Calibration of an 8-Pole Planar Radial Magnetic Actuator," ASME Paper 97-GT-18, *International Gas Turbine & Aeroengine Congress & Exhibition*, Orlando, Florida.

[5] Gahler C., 1998, "Rotor Dynamic Testing and Control with Active Magnetic Bearings," Ph.D. dissertation, ETH, Zurich, Switzerland.

[6] Knopf E., Nordmann R., 2000, "Identification of the Dynamic Characteristics of Turbulent Journal Bearings Using Active Magnetic Bearings," IMehcE Paper C576/110/2000.

[7] Pottie K., Matthijssen J., Norbart C., Gielen L., 1999, "Modal Parameter Estimation of Rotation Machinery," IMechE Paper C556/005/99.

[8] Raymer S., Childs D., 2001, "Force Measurements in Magnetic Bearings Using Fiber Optic Strain Gauges," ASME Paper 2001-GT-0027, *International Gas Turbine & Aeroengine Congress & Exhibition*, New Orleans, Louisiana.

[9] Pavesi L., Childs D., 2002, "Force Measurement in Magnetic Bearings using Fiber Optic Strain Gauges." MS thesis, Texas A&M University, College Station, Texas.